JBIC (1997) 2:652–661

ORIGINAL ARTICLE

John Fetter · Jonathan Cohen · Dana Danger
Joann Sanders-Loehr · Elizabeth C. Theil

The influence of conserved tyrosine 30 and tissue-dependent differences in sequence on ferritin function: use of blue and purple Fe(III) species as reporters of ferroxidation

Received: 12 March 1997 / Accepted: 16 July 1997

Abstract Ferritins uniquely direct the vectorial transfer of hydrated Fe(II)/Fe(III) ions to a condensed ferric phase in the central cavity of the soluble protein. Secondary, tertiary and quaternary structure are conserved in ferritin, but only five amino acid residues are conserved among all known ferritins. The sensitivity of ferroxidation rates to small differences in primary sequence between ferritin subunits that are cell-specifically expressed or to the conservative replacement of the conserved tyrosine 30 residue was demonstrated by examining recombinant (frog) H-type (red blood cell predominant) and M-type subunit (liver predominant) proteins which are both fast ferritins; the proteins form two differently colored Fe(III)-protein complexes absorbing at 550 nm or 650 nm, respectively. The complexes are convenient reporters of Fe(III)-protein interaction because they are transient in contrast to the Fe(III)-oxy complexes measured in the past at 310–420 nm, which are stable because of contributions from the mineral itself. The A650-nm species formed 18-fold faster in the M-subunit protein than did the 550-nm species in H-subunit ferritin, even though all the ferroxidase residues are the same; the Vmax was fivefold faster but the Hill coefficents were identical (1.6), suggesting similar mechanisms. In H-subunit ferritin, substitution of phenylalanine for conserved tyrosine 30 (located in the core of the subunit four-helix bundle) slowed ferroxidation tenfold, whereas changing surface tyrosine 25 or tyrosine 28 had no effect. The Fe(III)-tyrosinate was fortunately not changed by the mutation, based on the resonance Raman spectrum, and remained a suitable reporter for Fe(III)-protein interactions. Thus, the A550/650 nm can also report on post-oxidation events such as transport through the protein. The impact of Y30F on rates of formation of Fe(III)-protein complexes in ferritin, combined with Mössbauer spectroscopic studies that showed the parallel formation of multiple Fe(III) postoxidation species (three dinuclear oxy and one trinuclear oxy species) (A. S. Periera et al., Biochemistry 36:7917–7927, 1997) and the loss of several of the multimeric Fe(III) post-oxidation species in a Y30F alteration of human recombinant H-ferritin (E. R. Bauminger et al., Biochem J. 296:709–719, 1993), indicate that at least one of the pathways for Fe oxidation/transfer in ferritin is through the center of the four-helix bundle and is influenced by structural features dependent on tyrosine 30.

Key words Iron kinetics · Ferritin · Ferroxidase · Tyrosine modification · Raman spectroscopy

J. Fetter[1] · D. Danger[2] · E.C. Theil (✉)
Department of Biochemistry, North Carolina State University, Raleigh, NC 27695-7622, USA
Tel.: +1-919-515-5805; Fax: +1-919-515-5805;
e-mail: theil@bchserver.bch.ncsu.edu

Present addresses:
[1] Smith Kline Beecham, One Franklin Plaza, Philadelphia, PA 19101, USA
[2] Glaxo-Wellcome, 5 Moore Drive, Research Triangle Park, NC 27709, USA

J. Cohen · J. Sanders-Loehr
Department of Chemistry, Biochemistry, and Molecular Biology, Oregon Graduate Institute of Science and Technology, Portland, OR 97291-1000, USA

Introduction

Ferritin protein concentrates and stores iron, up to 4500 Fe/molecule, for use in many biochemical reactions. Twenty-four subunits in the form of hollow spheres direct iron to the protein interior where a solid phase of $Fe_2O_3(H_2O)_n$ forms. Subunit folding and packing are highly conserved in all ferritins, but sequence information now available shows that amino acid sequence is less highly conserved; only five amino acids are conserved in all known ferritins: two glycines at helix turns, an aspartic acid at the threefold subunit interface, a glutamic acid residue at position 103, and a tyrosine at position 30 [1]; glutamic/aspartic acid is aways present at position 57. Ferritin proteins which have fast rate of Fe uptake (oxidation and transfer to

the mineral) also have a single (ExxH) motif at residues 58–61 which may be homologous to the ExxH motifs for Fe at active sites in catalytic proteins [2], even though the Fe is a substrate in ferritin. In higher vertebrates, ferritin subunits associated with rapid Fe uptake are designated H-type and those with slow Fe-uptake are designated L-type. The effect of substitution of the E, H residues in the ExxH motif suggests an important role in the first step of Fe transfer through the ferritin protein, namely ferroxidation (reviewed in [2]). In vivo, long-term iron storage is associated with ferritins rich in L subunits and rapid iron turnover and/or higher oxygen concentration is associated with ferritins rich in H subunits.[1]

A third type of subunit, M, which is found in amphibians, is similar to H subunits in sequence, differing in only 19 amino acids in the frog H and 39 amino acids in the human H subunit, while retaining the ExxH motif and all other proposed Fe(III) ligands; most of the amino acid differences are conservative, e.g. V43I and T92S. M-type ferritin subunits predominate in liver ferritin and H-ferritin subunits in the red cells [3], emphasizing the biological importance of the different types of ferritin subunits. Natural ferritins are all hybrids of subunits, with tissue-specific differences in subunit ratios.

Many studies of ferritin structure and function have emphasized either the ligands involved in the first step in Fe transit across the protein, oxidation, or the last step, binding to the nucleation site [4–16]. However, the high conservation of quaternary structure in ferritin, which creates the large cavity (8-nm diameter) and facilitates the vectorial transfer of the Fe ions across the protein from outside to the cavity, suggests that other parts of the ferritin subunit, which may not be direct Fe ligands, can influence the oxidation/transit process.

To analyze Fe(III) oxidation and transit though the protein before formation of the bulk iron mineral, we have used colored species absorbing at 550 nm or 650 nm as reporters of the kinetics of Fe(III)-protein complex formation because they are transient and are not influenced by the absorbance of the stable mineral. Absorbance data (310–420 nm) collected in earlier papers do not decay with time because of the absorbance of mineralized Fe(III) species. Recent rapid-freeze quench Mössbauer spectroscopic studies show that after ferroxidation, but before formation of the mineral, multiple Fe(III) species form in parallel [three types of dimer and a trimer Fe(III) species] and appear to represent a series of alternative Fe(III) species in transit through the protein [39]. The rate of formation of the four-species multinuclear species parallels the formation of the A550-nm complex used here as reporter. [The A550-nm Fe(III) species is an Fe(III)-tyrosine [21, 22] apparently formed at one of the four other tyrosines in the molecule (36, 133, 147, 164) since Y30F, Y28F and Y25F all formed the Fe(III) tyrosinate; future identification of the tyrosine which is liganded to the Fe(III) will help define postoxidation sites of Fe(III) in transit through ferritin, but is outside the scope of this study.] In the present study, using the A550-nm species or the A650-nm species to monitor the kinetics of formation of Fe(III)-protein intermediates in frog H-ferritin or frog M-ferritin, respectively, we show the sensitivity of the kinetics of formation of Fe(III)-protein species to the substitution of conserved tyrosine 30[2] and to small (19/175 residues) differences in protein sequence of H- and M-ferritin subunits that are expressed tissue-specifically [3]. The multiplicity of fast rates of oxidation and absorbance of Fe(III) protein complexes possible in ferritin is now demonstrated by the data from the very similar types (H and M) of recombinant ferritin protein isolated and measured under identical conditions. Non-ligand amino acids in M and H subunits appear to have significant effects on rates of oxidation and absorbance spectra of initial Fe(III) complexes.

Materials and methods

Mutagenesis and protein isolation

The coding sequences for frog H and frog M subunits of ferritin were derived from pJD5F12 and pJD1D10 [3], respectively, and subcloned in a PET-3a expression vector. Mutagenesis was carried out using either the Stratagene Chameleon kit or by using PCR and primers for the different phenylalanine substitutions and the frog H-subunit cDNA [22] as the template. The DNA sequences were verified for each plasmid studied (*Escherichia coli* BL21-D3). Clones harboring single plasmid vector sequences were expanded and proteins isolated from the harvested cells as described in [22], except that in some later preparations betaine was omitted from the buffer for the Sepharose Q column. [Cells were cultured with betaine and sorbitol to minimize incorrect folding of the expressed ferritin subunits [24].] Yields of soluble protein varied from 85 to 10 mg/liter of culture, depending on the protein sequence. The iron content of the apoprotein as isolated was ≤ 5 Fe atoms/molecule as isolated from *E. coli.*

Kinetic data collection and analysis

Equal volumes of ferrous sulfate (1.96×10^{-4} M in 1 mM HCl containing 200 mM NaCl) and apoferritin (4.18×10^{-6} M) in 200 mM MOPS, 200 mM NaCl (pH 7.0) were mixed in an Applied Photophysics (APP) stopped-flow spectrophotometer, and data were collected in either the single wavelength or diode array mode. The Fe/protein ratio of 48 was selected to give the maximum formation of the A550- or A650-nm species as well as to increase the relative contribution of Fe(III) interacting with the protein compared to the inorganic phase [21]. Somewhat faster decay of the Fe(III)-tyrosinate was noted in the diode array mode, most probably because of photo-bleaching. Thus, the monochromator and

[1] H and L subunits have, at various times, been equated with tissue specificity or mass. It is now known that H and L sequences may have the same mass, albeit different mobility in denaturing gels (reviewed in 1 and 38) and can occur in many different tissues

[2] The numbering used in [17, 18, 23, 25] departs from the original numbering introduced for ferritin structures [8] by +4, making tyrosine 30 = tyrosine 34 in those papers

single-wavelength collection were used for kinetic analysis. For H-subunit ferritins, changes in absorbance at 550 nm were fit from 10 to 100 s for Y30F and from zero time to the time of maximum absorbance (3.5 or 9 s) for the parent protein. The data were analyzed using the APP global fitting package. In general, a double exponential gave twofold to fourfold better fits, likely due to the contribution of the "burst" phase to the reaction. The normalized variance ($\times 10^6$) were 1.79 for the single exponential and 0.451 or 0.479 for double exponential fits of Y30F and the parent protein, respectively. For the M-subunit ferritin, data for both the rapid formation and rapid decay at 650 nm were fit to a double exponential with a normalized variance of 1.49×10^{-6}.

Resonance Raman (RR) spectroscopy

Samples of wild-type and mutant proteins (3 mM in subunits) containing Fe(II) at a ratio of 48 Fe atoms/protein molecule were prepared in 100 mM bistris-propane, 250 mM NaCl (pH 7.5). Similar RR spectra were obtained in MOPS buffer. As before [22], the 550-nm intermediate was formed by adding Fe(II) to an anaerobic solution of apoprotein purged for 1 h with argon, followed by exposure to air for 5 min. At this point, samples were transferred to glass capillary tubes which were flame sealed and frozen with dry ice. The samples were thawed immediately before data collection. Raman spectroscopy was performed on a custom-built McPherson 2061/207 Raman spectrograph equipped with an 1800-groove/mm holographic grating, a Princeton Instruments LN1100PB liquid N_2–cooled CCD detector, a Kaiser Optical Systems holographic super-notch filter, and interfaced to a Gateway 2000 personal computer. Excitation was provided by a Coherent Innova 90 Ar laser operating at 514.5 nm (50 mW). Interfering plasma emissions were removed with an Applied Photophysics prism monochromator. Spectra were recorded using 90 scattering geometry and 4-cm^{-1} resolution with the samples cooled to ~15 °C in a copper cold finger placed in a Dewar flask filled with cold water. All spectra were calibrated against indene or toluene as external standards for peak positions. Reported frequencies are accurate to 2 cm^{-1}. Spectra were smoothed and baselines corrected using GRAMS/386 (Galactic Industries) software.

Results

Protein engineering of H-ferritin

Tyrosine at position 30 (in the core of the subunit four-helix bundle) is found in all ferritins [1]. All eukaryotic ferritins have a tyrosine at position 28 (near the dimer interface)[2] (Fig. 1). Y28 appears to be solute-accessible based on its hydrogen bonding to solvent-derived betaine [12] and its proximity to the heme-binding site in bacterioferritin and horse spleen ferritin [19, 10]. Y30 is buried and is part of a stacked set of aromatic residues [10].

The tyrosine-encoding sites in the DNA of the frog H subunit were altered by single-site mutagenesis to encode phenylalanine at position 28 or 30, which are conserved tyrosines in all ferritins (Fig. 1). In addition, Y25, characteristic of H subunits and in a cluster with Y28 at the dimer interface of the assembled protein, was also changed to phenylalanine in a separate clone. A triple mutant containing Y25F, Y28F, and Y30F was also prepared, but the protein was in an inclusion body under a variety of *E. coli* growth conditions, and as yet has not been studied. Mutagenesis for the triple mutant was also difficult, requiring alternate phenylalanine codons.

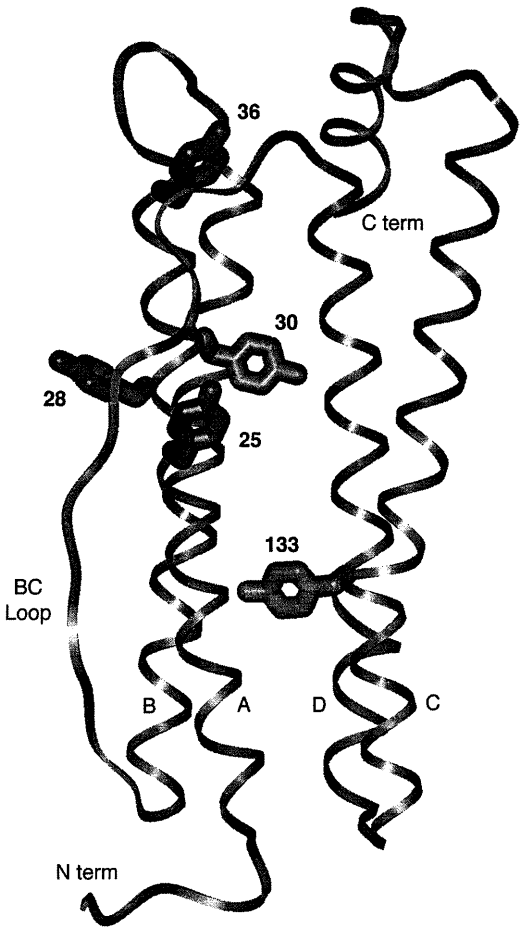

Fig. 1 Position of tyrosine residues in the H subunit of ferritin. This figure was composed from the coordinates for recombinant human H-subunit ferritin that had been crystallized with $CaSO_4$ [17]. The data were retrieved from the Brookhaven Protein Data Base (1FHA, P. Artymiuk and P.M. Harrison), graphically presented using Insight II, version 95.0 (Molecular Simulations), and corrected for a difference in numbering (see footnote 2 on p. 653)

The phenylalanine substitutions were introduced into a variant of the frog H-ferritin subunit, L134P, which is expressed well in *E. coli.* Not enough of the frog H wild-type sequence (L134) can be expressed to analyze. The site of the variation is the D helix and should have little effect on ferritin function based on current knowledge. Similar arguments have been used to justify the examination by crystallography, Mössbauer spectroscopy and UV-vis spectroscopy of the human H variant K86Q or CdM (e.g. [17, 18, 23]).

The L134P mutation does not seem to have affected the function of frog H ferritin since both frog H (L134P) and human H share the long lag required to restore the initial rate of ferroxidation [21, 23] and both proteins display a similar set of heterogeneous Fe(III) species, which are precursors to the mineral, when analyzed by Mössbauer spectroscopy [18, 25]. Two addi-

tional observations minimize the likelihood that the L134P effect will be large. First, a crystal structure of the frog L protein, which has a proline at position 132 near to position 134 shows almost no distortion in the backbone at the proline compared to the structure of the human H subunit which has no proline in the region [12]. Second, studies on T4 lysozyme show that proline substitution does not necessarily make large alterations in structure or function (40) especially in helices. Thus, the frog H (L134P) which was used as the parent clone for the mutagenesis in this work is simply referred to here as frog H-ferritin.

Fe(III)-tyrosinate as a ferroxidase reporter in H ferritin

When frog H-subunit apoferritin is reacted with a two-fold excess of Fe(II) per subunit and O_2, it rapidly forms a purple complex with an absorbance maximum at 550 nm (Fig. 2). For the first time, the A550-nm species made possible the study of the kinetics of an Fe(III)-protein complex without confounding contributions from polynuclear Fe(III) species and bulk mineral. Differences in the kinetics of measurements at 330 nm and 550 nm have been clearly demonstrated [23]. Later, a different species absorbing at 650 nm was observed to form in other fast ferritins: human H-K86Q [23] and frog M (Fig. 2), possibly due to a peroxide or tyrosinate complex. The nature of this species has not yet been determined because of the difficulty in trapping the species at high enough concentrations for RR measurements. But the A550-nm species in the frog H-subunit ferritin has been definitively identified as an Fe(III)-tyrosinate from the appearance of a characteristic RR spectrum (Fig. 3), with maximum intensity upon excitation within the 550-nm absorption band [22]. Thus, this Fe(III) complex provides a useful means for monitoring iron oxidation. Its RR spectrum exhibits five features that can be assigned to iron-tyrosinate vibrations: two ν(C-O) stretching modes at 1287 and 1300 cm^{-1}, two ν(C-C) stretching modes at 1501 and 1600 cm^{-1}, and a δ(C-H) bending mode at 1169 cm^{-1} (Fig. 3). These assignments are based on the strong similarity to the RR spectra of model compounds of known structure containing iron-phenolate groups [31].

The Fe(III)-tyrosinate in ferritin shares RR spectral features with other iron-tyrosinate proteins (Table 1). For example, the RR spectrum of catechol 1,2-dioxygenase (CTD) reveals four bands assigned to Fe(III)-tyrosinate vibrations: two ν(C-C) at 1604 and 1506 cm^{-1}, a broad ν(C-O) at 1289 cm^{-1}, and a δ(C-H) at 1175 cm^{-1} [26]. Similar iron-tyrosinate vibrations are observed in bacterial protocatechuate 3,4-dioxygenase (PCD) [27] and bovine purple acid phosphatase [28]. However, the RR spectrum of the Fe(III)-tyrosinate in frog H-subunit ferritin is somewhat unusual in that the C-O stretching region contains two distinct peaks at 1287 and 1300 cm^{-1}. The enzyme PCD also has two

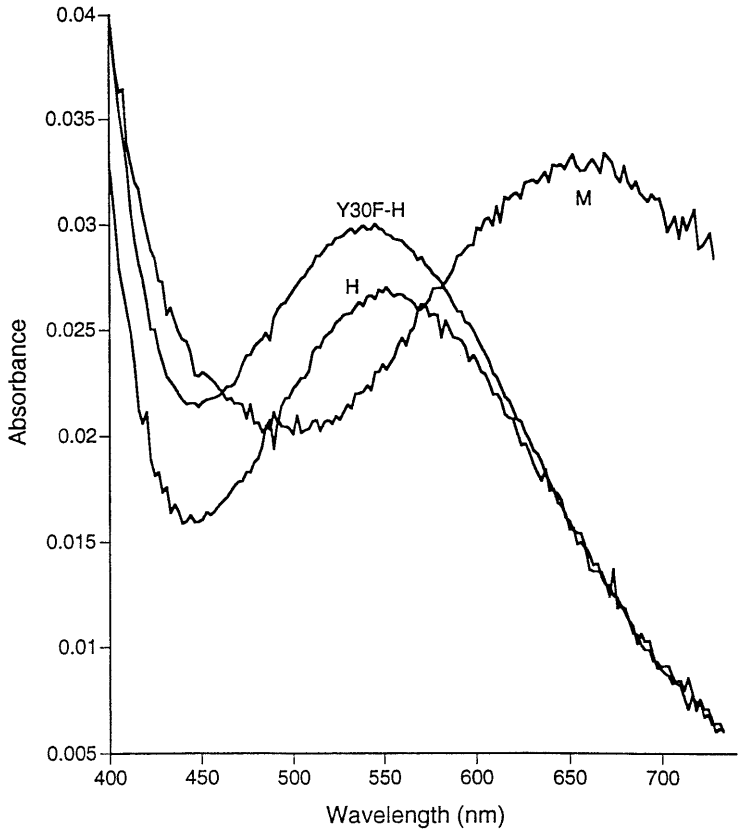

Fig. 2 UV-VIS spectra of fast-mineralizing recombinant frog ferritins. Diode-array spectra were recorded at the time of maximum color formation, 4.1 s for H-subunit ferritin, 17 s for the Y30F mutant of H-subunit ferritin, and 0.09 s for the M-subunit ferritin (see Table 2)

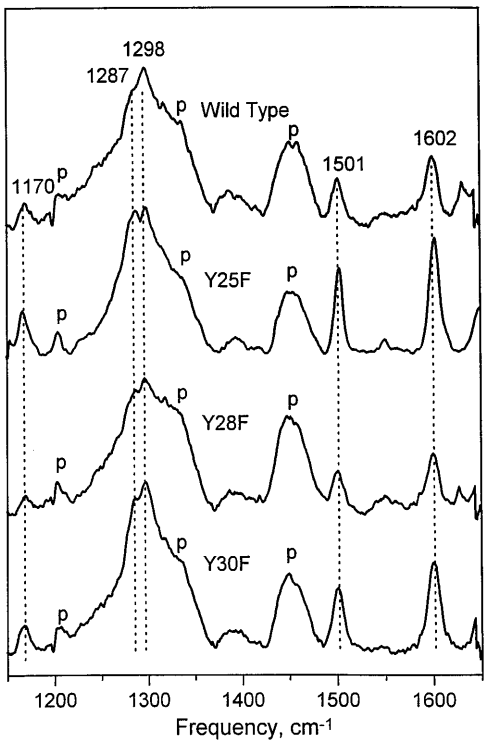

Fig. 3 Resonance Raman spectra of the A550-nm complex in recombinant frog H-subunit ferritin and its Y to F mutants at positions 25, 28, or 30. Samples were prepared by anaerobic addition of $FeSO_4$ (48 Fe/protein), followed by 5-min exposure to air. Non-enhanced Raman modes of the protein are denoted by p. Similar resonance raman spectra were obtained after 40-s exposure to air

such ν(C-O) modes (Table 1) that have been assigned to the separate contributions of the equatorial and axial tyrosinate ligands to Fe(III) seen in the crystal structure [29]. The relative RR intensities of the two ν(C-O) modes in PCD change with excitation wavelength, as expected for two tyrosines with different Tyr Fe(III) charge transfer transitions [27]. Furthermore, one of the C-O vibrational frequencies is preferentially perturbed by D_2O (indicative of H bonding) or by binding of the inhibitor 4-hydroxybenzoate (Table 1). The two ν(C-O) modes in frog H ferritin show no change in relative intensities at different excitation wavelengths, suggesting they are more likely due to a single tyrosinate ligand.

The efficacy of using formation of the Fe(III)-tyrosinate as a reporter for ferritin ferrokinetics in the altered proteins is shown in Figs. 2 and 3. A similar approach was attempted in the human H ferritin-K86Q, Y30F protein [23], but neither the A650-nm species nor an A550 species was observed, and measurements could only be made at 330 nm, where bulk and polynuclear Fe(III)-oxo complexes contribute significantly to the spectrum; no detailed kinetic data were collected [23]. The Fe(III) complexes of the Y25F, Y28F, and Y30F mutants all exhibited the absorbance with a maximum at 550 nm (shown for Y30F in Fig. 2) and the same quantitative absorbance intensity as in the frog H-ferritin progenitor. The RR spectra were also unchanged by the phenylalanine substitutions, retaining two ν(C-O) vibrations at $\sim$1287 and $\sim$1298 cm^{-1}, two ν(C-C) modes at $\sim$1502 and $\sim$1602 cm^{-1}, and a δ(C-H) mode at $\sim$1170 cm^{-1} (Fig. 3, Table 1). The possibility existed that substitution of phenylalanine for tyrosine would simplify the RR spectrum if the spectral splitting of ν(C-O) had been due to different conformations of the protein or to the participation of multiple tyrosine residues. However, the same spectral splitting occurred in the parent protein and in all three mutants, and the relative intensities of the two ν(C-O) modes were unaffected by varying the protein preparation, temperature, or reaction time (factors which all should be sensitive to protein conformation).

An alternative explanation for the ν(C-O) splitting in the Fe(III)-tyrosinate spectrum of frog H subunits is Fermi resonance. According to this phenomenon, a single ν(C-O) mode would couple with another tyrosine ring vibration of the same energy to produce a doublet of peaks at higher and lower energy. Tyrosine has long been known to exhibit a Fermi doublet at 830 and 850 cm^{-1}, and these two modes are typically observed in the Raman spectra of all tyrosine-containing proteins [30]. Since the frequency of ν(C-O) varies from 1265–1310 cm^{-1} depending on the nature of the protein envi-

Table 1 Raman vibrational frequencies (in cm^{-1}) for ferric-phenolate complexes in proteins

Protein complex[a]	δ(C−H)	ν(C−O)	ν(C−C)	ν(C−C)
Frog ferritin H	1169	1287/1300	1501	1600
Frog ferritin Y25F-H	1167	1287/1297	1501	1603
Frog ferritin Y28F-H	1170	1288/1297	1501	1601
Frog ferritin H Y30F-H	1170	1288/1297	1504	1604
Catechol 1,2-dioxygenase	1175	1289	1506	1604
Protocatechuate 3,4-dioxygenase (PCD)	1176	1254/1266	1505	1605
PCD + (4-OH)benzoate[b]	1174	1256/1288	1505	1606
Purple acid phosphatase	1164	1281	1497	1597

[a] Frog H subunits contain a spontaneous L134P mutation in both the parent and the Y30F derivative that is apparently related to high expression. Data are taken from the following references: Frog ferritin H ([22] and Fig. 3); frog ferritin derivatives (Fig. 3); catechol 1,2-dioxygenase [26]; PDC (protocatechuate 3,4-dioxygenase) [27]; purple acid phosphatase [28]

[b] ν(C−O) of 4-hydroxybenzoate bound to Fe in PCD is 1276 cm^{-1} [27]

ronment [31], the occurrence of Fermi splitting would be more variable depending on the degree of overlap of vibrational frequencies in this region. In the case of frog H ferritin, the Fermi resonance appears to have been destroyed by a shift in the frequency of ν(C-O) in D_2O, with the result that only a single intense ν(C-O) was observed at 1287 cm^{-1}. Regardless of the origin of the C-O vibrations, the unusual Fe(III)-tyrosinate moiety in frog H ferritin serves as an excellent reporter for the rapid ferroxidation pathway.

Influence of Tyr 30 on the kinetics of ferroxidation

Tyrosine 30 has previously been proposed to play a role in the rapid ferroxidation of H-subunit ferritin [23]. These authors found that the Y30F mutation in human H-K86Q ferritin caused slower iron uptake, as measured by 1,10-phenanthroline binding to remaining Fe(II), and a longer lag time in the appearance of the 330-nm-absorbing product which is a mixture of early Fe(III)-protein complexes, polynuclear and bulk mineral Fe(III) species; unfortunately, in the human H Y30F variant, the A650 nm species could not be detected, and so no detailed kinetic data were collected. In contrast, the retention of the A550-nm reporter in the frog H, Y30F mutation allowed the measurement of the rates of formation of the A550-nm reporter by stopped flow spectrophotometry (Fig. 4). Although the Y30F mutant formed a similar amount of the intermediate based on the calculated absorbance intensity at 550 nm (Table 2), the rate of formation was considerably slower than in the frog H-subunit progenitor (Fig. 4). The parent protein exhibited maximum absorbance in 6 s and then began to decay, whereas the Fe(III)-tyrosinate complex had barely begun to form in the Y30F mutant in this same time period. The rates of Fe(III)-tyrosinate formation were computed in the range 10 ms to 200 s and were well fit by either a one- or two-exponential expression (see Methods). For the Y30F mutant, the initial rate (within the first 200 ms) was four times slower than the parent H subunit and the half-life ($t_{1/2}$) for the major phase of the process was 11 times longer, leading to a lag in complex formation such that the time until maximum Fe(III)-protein complex formation was 25 times longer (Table 2). These results explain the previously observed persistence of Fe(II) in the Mössbauer spectrum of the Y30F mutant of human H ferritin [18] and provide definitive evidence that Tyr 30 participates in the rapid ferroxidation pathway.

The nearby tyrosines at positions 25 and 28 behaved very differently from Tyr 30. The Y25F and Y28F mutants of frog H-ferritin were indistinguishable from the parent protein in the kinetics of formation of the Fe(III)-tyrosinate species with absorbance at 550 nm (data not shown). Similarly, the Y25F and Y28F mutants of human H ferritin were similar to parent protein in the rate of production of the 330-nm oxidation product [23].

A650-nm species as a ferroxidase reporter in frog M-subunit ferritin

In frogs there are two types of fast ferritin subunits (H and M). H is predominant in red blood cell ferritin and

Table 2 Kinetics of formation of Fe(III) complexes in recombinant apoferritins[a]

Parameter[b]	Y30F-H subunit	H subunit	M subunit
$t_{1/2}$ for formation of major phase (s)	12.3 ± 1.2	1.1 ± 0.4	0.028 ± 0.003
Absorbance intensity	0.030 ± 0.005	0.026 ± 0.002	0.056 ± 0.005
Initial rate (AU/sec)	0.020 ± 0.013	0.081 ± 0.038	1.55 ± 0.22
V_{max}	–	0.85 ± 0.06[c]	4.31 ± 0.17
n	–	1.6 ± 0.1[c]	1.6 ± 0.1
Time to maximum formation (s)	130 ± 20	6 ± 2	0.082 ± 0.006

[a] Frog H subunits contain a spontaneous L134P mutation in both the parent and the Y30F derivative that is apparently related to high expression. The rate of formation of Fe(III) complexes was measured at 550 nm for frog H subunits and at 650 nm for frog M subunits. Two independent preparations of protein were used and 2–6 independent sets of measurements were made for each type of protein. The error is shown as the standard deviation. Data were fit using the Applied Photophysics algorithms with the indicated function and fit range (see Methods)

[b] *$t_{1/2}$ for the second major phase (s)* Fitting for H subunit data used a double exponential equation from time 0 to the time the maximum absorbance was reached. For the M subunit, a double exponential equation was used to fit both the rapid formation and rapid decay from 0–5 s

Absorbance intensity The maximum of amplitude was determined from the kinetic fits

Initial rate (AU/sec) Fitting with a single exponential equation was used in the range was 0.006–0.1 s for M subunit data and 0.01–0.2 s for the slower H subunit data. The initial rate displayed much greater variation than the major second phase for which $t_{1/2}$ was computed

[c] Data taken from ref. 22

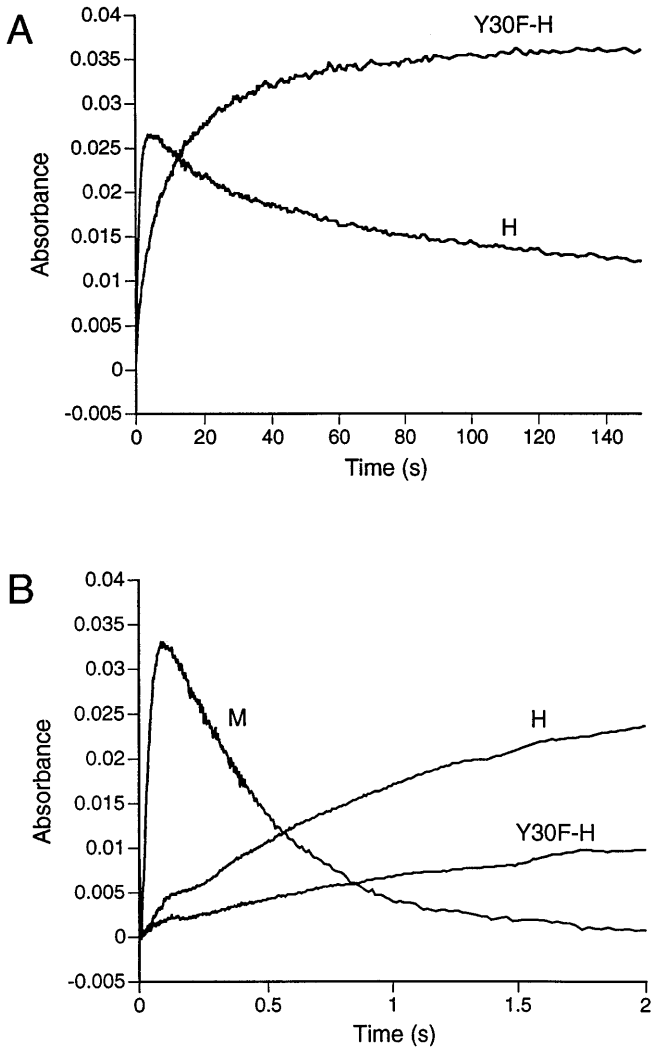

Fig. 4A,B Kinetics of formation and decay of the initial Fe(III)-protein complex in recombinant frog ferritins. Recombinant apoferritin (4.16×10^{-6} M in 200 mM MOPS, 200 mM NaCl, pH 7.0) was mixed with an equal volume of $FeSO_4$ (1.96×10^{-4} M in 200 mm NaCl, 1 mM HCl) in a stopped flow apparatus, and the absorbance was monitored with time. **A** Change in absorbance at 550 nm in H-subunit parent and Y30F derivative within the 200-s period used for the determination of rate constants (Table 2). **B** Change in absorbance at 550 nm in H-subunit parent and Y30F derivative and at 650 nm in M subunit within the first 2 s after mixing

M is predominant in liver ferritin [3]. (Whether or not there are two types in humans, for example, is not clear, since only two genes have been cloned. There are more than 30 hybridizable sequences in humans, only some of which have been examined, and hybridization experiments done on different cells would not distinguish between two ferritin subunits as similar as the frog H and M [38]).

H and M ferritin subunits differ in only 19 amino acid residues out of 175. The differences are throughout the subunit and often involve very conservative changes: M/H: Y8F, S10R, V16I, S31L, Y35F, F36Y, V42I, F65L, V68D, V76I, I81V, G91S, L116V, A117G, T118S, S131T, D140D, R143Q, F147Y.

Recombinant protein composed of the frog M subunit forms the A650-nm complex that is also observed in the human H-K86Q protein (Fig. 2 and [23]) rather than the A550-nm complex observed in the frog H subunit (Fig. 2). However, the frog M differs from the human H in twice as many sites (39 residues different) as does the frog H (19 residues different). Sequence comparison of the three subunits [1, 3] do not provide an obvious explanation of the differences in the Fe(III)-protein complexes.

Equally important is the effect of the sequence differences on the kinetics of ferroxidation in the frog H- and M-type ferritins. Striking differences occur in rates of formation and decay of initial Fe(III) species in frog H and M subunit ferritin (Figs. 4 and 5); the blue (A650-nm) complex forms and decays much more rapidly in the M subunit ferritin than the A550-nm complex in the H subunit ferritin (Fig. 5), although, when discovered, the A550-nm complex was the fastest reaction known in ferritin [21]. A difference of 18-fold in the rate of the initial phase is observed (Figs. 4 and 5, Table 2) and the Vmax is 5-fold higher (Table 2). Nevertheless, the cooperativity of the reaction is identical for the frog H and M proteins; ($n = 1.6$) (Table 2), and the overall effect of changing the number of added Fe(II) atoms/protein is comparable (Fig. 5), suggesting similarity of mechanisms.

Thus, small differences in mainly hydrophobic residues throughout the ferritin subunit have significant effects on the kinetics of ferroxidation, on the decay of the initial species (Fig. 4), and on the structure of the initial complex. (Note that the frog M subunit has an initial rate of ferroxidation about fourfold faster than the wild-type human H ferritin [J. Fetter, S. Torti and E. C. Theil, unpublished observations]). The tissue-specific differences in expression of the H and M types of ferritin subunits [3] suggest that the differences in ferritin Fe kinetics are physiologically significant.

Discussion

Mechanisms of ferroxidation

Hydrated ferric oxides which form inside of the ferritin protein can also form in a completely inorganic environment. Thus, the main function of ferritin is to concentrate and sequester iron as a condensed ferric phase. The protein serves to direct the vectorial transfer of the metal ions from the exterior surface to a central cavity. Oxidation of Fe(II) by the protein facilitates the rate of mineralization and is especially fast in proteins with a large amount of the H-type subunit. Identifying how the protein controls the mineralization and determining the molecular and biological significance of the differences in ferritin H- and L-subunit sequences remain major challenges.

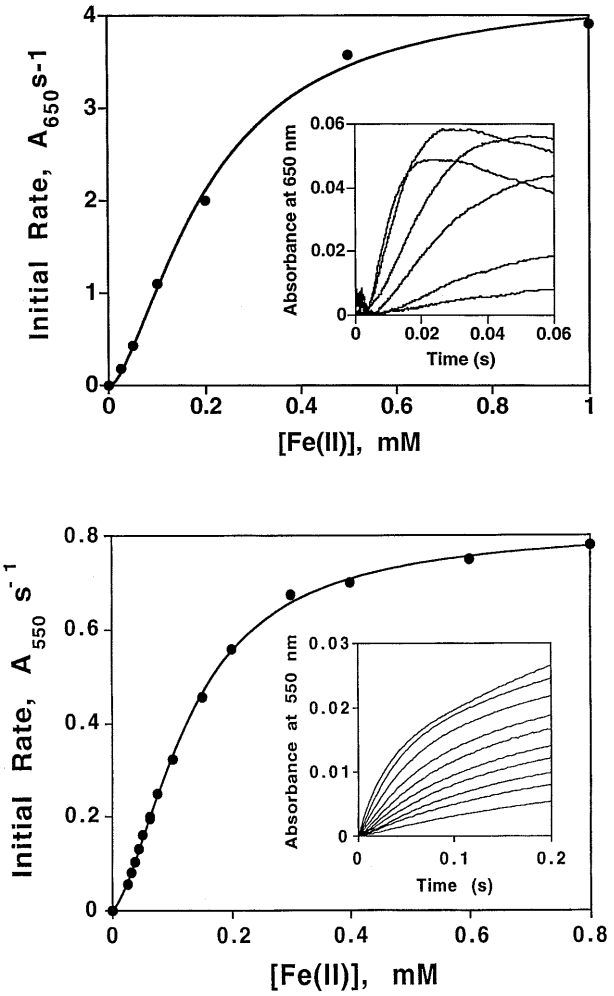

Fig. 5A,B Effect of varying Fe(II) concentration on initial rates of ferroxidation measured by the 650-nm species of bullfrog M ferritin compared to the 550-nm species of bullfrog H ferritin that has been characterized as an Fe(II) tyrosinate [21, 22]. Ultraviolet-visible stopped-flow kinetics were carried out as described in Fig. 4. **A** Initial rates for the bullfrog M were determined at Fe to protein molar ratios of 12, 24, 48, 96 and 240 and 480. Linear regression was used to fit the initial rates with the length of the fit varying from 5 to 30 ms depending on the rate. A nonlinear curve fit of the rates versus Fe(II) concentration of the Hill equation was calculated in Axum 4.0 to determine Vmax, *n*, and *K*. **B** Initial rates for the more slowly forming 550-nm species of bullfrog H ferritin were previously determined at Fe-to-protein molar ratios of 12, 18, 24, 36, 48, 72, 96, 192, 288, 384 [21]

The known steps which Fe ions take during mineralization of ferritin in solution are shown in Eqn 1.

$$\underset{\text{In solution}}{Fe(II)(H_2O)_6} \rightarrow \underset{\text{Transport intermediates}}{Fe(III)\text{-protein}} \xrightarrow[\uparrow]{H^+,H_2O} \underset{\text{Solid in protein cavity}}{Fe_2O_3(H_2O)_n} \quad (1)$$

Several protein sites are likely to be involved in the oxidation and movement of Fe atoms across the protein to the sites for nucleation of the mineral core because of the multiplicity of observed intermediates. A series of sites of increasing stability for Fe(III) mononuclear or multinuclear Fe(III)-oxo complexes could easily account for the vectorial movement of the iron ions across the protein.

Ferroxidation sites in ferritins are not fully understood. For L-subunit (slow) ferritins, in particular, chelation could play an important role [32–34]. Such a chelation site can be formed by the clusters of conserved Glu at the nucleation site where iron begins to assemble into a core-type polymer. Each L subunit contains several carboxylate ligands at the inner side of the dimer interface facing the cavity that have been identified as nucleation sites by mutagenesis and/or structure/function analysis of L-subunit ferritins [8, 9, 13, 25, 35, 36]. Substitution of alanine for glutamic acid at these sites slows ferroxidation [1, 9], with little change in protein structure except in the ordered water [12]. These results suggest a coincidence of nucleation and ferroxidation, at least in L-subunit ferritin. Similar conclusions have been drawn from the modification of carboxylate ligands in horse spleen ferritin (85–90% L subunits) or recombinant horse L ferritin [14, 37]. Since the same glutamate residues are conserved in both L and H subunits, it is likely that these carboxylate clusters serve as mineral nucleation sites in both types of ferritins.

The H-subunit (fast) ferritins clearly having additional sites within the protein which facilitate iron uptake and oxidation at up to 1000 times the rate in L-subunit ferritins [1]. These reactions were initially followed using the absorbance at 310–420 nm as a spectroscopic reporter for the formation of polymeric Fe(III)-oxo species. However, this measurement encompasses core nucleation and, thus, cannot yield specific information on the ferroxidation process. Recently it was discovered that fast ferroxidation could be monitored in frog H-subunit ferritins from the formation of an endogenous Fe(III)-tyrosinate intermediate with an absorbance at 550 nm [22]. This allowed investigation of the earlier stages of fast, H-subunit reactions which were shown to involve a burst followed by a slower decay and a very slow restoration of the initial site [21]. Similar results were obtained with an Fe(III)-protein complex that absorbs at 650 nm in the human H K86Q ferritin [23], but loss of the complex in the Y30F variant made analysis of ferroxidaition difficult to measure, and no quantitative kinetic data were collected [23].

Role of tyrosine 30

Of the three tyrosine residues studied by phenylalanine substitution, the conserved Y28 and Y30 and the H-subunit-specific Y25, only the Y30F mutation had any effect on the ferroxidation kinetics of frog H-subunit ferritin (Fig. 4, Table 2). Tyrosines 25 and 28 occupy positions on the subunit surface facing the dimer interface and, based on the interaction with solute betaine in protein crystals, are accessible to the solvent [12]. In

contrast, Tyr 30 faces the center of the subunit four-helix bundle and participates in a stack of aromatic residues contributed by several helices [11]. The side-chain of Tyr 30 could, thus, function either in the stabilization of subunit structure, or in electron transfer (H- or L-subunit ferritins), or in fast (H-subunit-specific) ferroxidation as a ligand to Fe(III). Y30 is close to the site in the middle of the subunit four-helix bundle that forms stable complexes with metals (Tb, Ca, Fe) and has been proposed to be a major site for ferroxidation [2, 17, 18].

Mechanistic studies of ferritin mineralization are insufficiently advanced at this time to distinguish definitively among the several roles possible for Y30. Ferroxidation is only one of the requirements. Transfer of electrons, paths of proton exit, and paths of Fe(III) transport have barely begun to be explored. Earlier concepts of a rigid protein pierced by fixed channels of several types through which hydrated Fe ions passed have had to be reevaluated in the light of new data. For example, the fourfold channel is not present in the crystal structure of functional frog L-subunit ferritin [11], crystallization conditions and amino acid substitutions have been shown to have marked effects on side-chain conformation and ordered water [12], and the lag in restoration of the ferroxidation site compared to decay of initial Fe(III)-protein complexes indicates the presence of alternative protein conformations [1, 22, 23]. Furthermore, multiple Fe(III)-oxy species have been observed by fixed-time Mössbauer spectroscopy at 1 min when essentially all of the Fe(II) was oxidized [18, 25]. Using rapid-freeze quench in combination with high-field Mössbauer spectroscopy, this multiplicity of Fe(III)-oxy species has been found to be present at the earliest observable stages of the reaction (25 ms) when only 50% of the Fe(II) has been oxidized [39]. This raises the possibility of multiple simultaneous fast ferroxidation sites.

H versus M ferritin and cell-specific ferritin subunits

The major differences in cell-specific expression of ferritin subunits has concerned the slow L type and the fast H types. In frogs and possibly other species such as the pig (reviewed in [38]), there are two types of fast-ferritin subunits that are expressed cell specifically [3]. The data in Figs. 4 and 5 and Table 2 show the functional consequences of the 19 amino acid substitutions in the frog M-ferritin subunit, compared to the frog H subunit. An Fe(III)-protein complex forms in M-subunit ferritin, which has a large (100-nm) shift in the absorbance maximum to the blue compared to that of the H-subunit ferritin. Potential Fe(III) complexes absorbing at $\sim$650 nm include Fe(III)-tyrosinate and Fe(III)-peroxo species. The rate of formation of the blue Fe(III) complex in the frog M subunit is 18-fold faster than the purple Fe(III) complex in the frog ferritin H subunit, the Vmax is fivefold higher and the decay is so fast (Figs. 4 and 5) that not enough has yet been trapped to identify. On the other hand, all three recombinant ferritins studied so far (frog H, L134P; human H, K86Q; frog M) show cooperativity of the Fe(III)-protein interaction with a Hill coefficient of 1.6 (Table 2 [22, 23]) indicating similar mechanisms for all the ferritin subunit types with the rate/affinity being the subunit-specific variable. The Hill coefficient has been interpreted as indicating that a pair of Fe atoms are involved [23]. However, the Mössbauer data showing that Fe(III) trimers and dimers form at the same rate [39] suggest that an alternative explanation is needed, such as protein-protein interactions or dioxygen/Fe binding to account for the observed cooperativity.

What is clear from the data is that amino acids which influence ferroxidation in ferritin may be involved in stabilization of subunit structure through stacking of aromatic residues (in which Y30 participates) or hydrogen bonding (which would be disrupted in Y30F) and need not be direct ligands to the Fe. A structural role for Y30 is suggested by the fact that it is a conserved residue in both H and L chains. Further evidence for the indirect influence of protein structure on ferroxidation is provided by the effect of the 19 relatively conservative changes between the H an M frog ferritin subunits [3], the relatively low level of conservation of primary sequence now apparent [1], the fast ferroxidation by bacterioferritin [41], which diverges so much from vertebrate ferritins in primary sequence that any relationship was initially undetectable [42], and by the recent helix exchange experiments with human and mouse H-subunit ferritin in which amino acids at positions 132, 135, 140 and 161 were shown to influence ferroxidation [16]. Because the ferritin subunits function in an assembly with a highly specific and conserved quaternary structure, small changes at a single site in a subunit could be amplified in the 24-subunit protein. Past emphasis on the conservation of *specific Fe-binding residues* in subunits related to oxidation sites may have obscured the role of *regions* of the protein in ferrokinetics, indicated by the functional effects of relatively conservative changes in amino acid sequence displayed by the frog H- and M-subunit recombinant ferritins (Figs. 4 and 5). Genetic regulation of the frog H- and M-ferritin subunits is so precise [3] that the functional differences observed here are likely to be physiologically significant. The finding that the internal Tyr 30 influences rapid uptake of iron in H-subunit ferritins lends support to the hypothesis [17] that residues in a central region of the subunit four-helix bundle are involved in fast ferroxidation.

Acknowledgements The authors are grateful to Dr. Geoffrey S. Waldo for making the phenylalanine/tyrosine substitutions in frog H-subunit ferritin, to Trista Schagat for subcloning the M subunit into pet3a, to Dr. Jinshu Ling for determining the excitation- and md-dependence of the RR spectra, and to Prof. Carol Fierke for extensive and extremely helpful discussions on the kinetic analysis of Fe(II) oxidation by H-subunit ferritins. This work was supported by research grants from the National Institutes of Health (DK 20251 to E.C.T. and GM 18865 to J.S.-L.) and an American Heart Association Fellowship (J.F.).

References

1. Waldo GS, Theil EC (1996) In: Suslick KS (ed) Comprehensive supramolecular chemistry, vol 5. Pergamon, Oxford, pp 65–89
2. Harrison PM, Arosio P (1996) Biochim Biophys Acta 1275:161–203
3. Dickey LF, Sreedharan S, Theil EC, Didsbury JR, Wang Y-H, Kaufman RE (1987) J Biol Chem 262:7901–7907
4. Rohrer JS, Joo M-S, Dartyge E, Sayers DE, Fontaine A, Theil EC (1987) J Biol Chem 262:13385–13387
5. Rohrer JS, Frankel RB, Papaefthymiou GC, Theil EC (1989) Inorg Chem 28:3393–3395
6. Yablonski MJ, Theil EC (1992) Biochemistry 31:9680–9684
7. Treffry A, Harrison PM (1979) Biochem J 181:708–716
8. Rice DW, Ford GC, White JL, Smith JMA, Harrison PM (1983) Adv Inorg Biochem 5:39–50
9. Wade VJ, Levi S, Arosio P, Treffry A, Harrison PM, Mann S (1991) J Mol Biol 221:1443–1452
10. Trihka J (1994) PhD thesis, Wesleyan University, Middletown, CT, USA
11. Trikha J, Waldo GS, Lewandowski FA, Theil EC, Weber PC, Allewell NM (1994) Proteins 18:107–118
12. Trihka J, Theil EC, Allewell NM (1995) J Mol Biol 248:949–967
13. Mertz JR, Theil EC (1983) J Biol Chem 258:11719–11726
14. Crichton RR, Herbas A, Chavez-Alba O, Roland F (1996) J Biol Inorg Chem 1:567–573
15. Levi S, Santambrogio P, Cozzi A, Rovida E, Corsi B, Tanborini E, Spada S, Albertini A, Arosio P (1994) J Mol Biol 238:649–654
16. Rucker P, Torti FM, Torti SV (1996) J Biol Chem 271:33352–33357
17. Lawson DM, Artymiuk PJ, Yewdall SJ, Smith JMA, Livingstone JC, Treffry A, Luzzago A, Levi S, Arosio P, Cesareni G, Thomas CD, Shaw WV, Harrison PM (1991) Nature 349:541–544
18. Bauminger ER, Harrison PM, Hechel D, Hodson NW, Nowik I, Treffry A, Yewdall SJ (1993) Biochem J 296:709–719
19. Frolow F, Kalb (Gilboa) AJ, Yariv J (1994) Nature Struct Biol 1:453–460
20. Precigoux G, Yariv J, Gallois B, Dautant A, Courseille C, D'Estaintot LB (1994) Acta Crystallogr, Sect D 50:739–743
21. Waldo GS, Theil EC (1993) Biochemistry 32:13261–13269
22. Waldo GS, Ling J, Sanders-Loehr J, Theil EC (1993) Science 259:796–798
23. Treffry A, Zhao Z, Quail MA, Guest JR, Harrison PM (1995) Biochemistry 34:15204–15213
24. Blackwell JR, Horgan R (1991) FEBS Lett 295:10–12
25. Bauminger ER, Harrison PM, Hechel D, Nowik I, Treffry A (1991) Biochim Biophys Acta 1118:48–58
26. Que L Jr, Heistand RH II, Mayer R, Roe AL (1980) Biochemistry 19:2588–2593
27. Siu DC, Orville AM, Lipscomb JD, Ohlendorf DH, Que L Jr (1992) Biochemistry 31:10443–10448
28. Averill BA, Davis JC, Burman S, Zirino T, Sanders-Loehr J, Loehr TM, Sage JT, Debrunner PG (1987) J Am Chem Soc 109:3760–3767
29. Ohlendorf DH, Orville AM, Lipscomb JD (1994) J Mol Biol 244:586–608
30. Siamwiza MN, Lord RC, Chen MC, Takamatsu T, Harada I, Matsuura H, Shimanouchi T (1975) Biochemistry 14:4870–4876
31. Que L Jr (1988) In: Spiro TG (ed) Biological applications of resonance Raman spectroscopy, vol 3. Wiley, New York, pp 491–521
32. Sun S, Chasteen ND (1992) J Biol Chem 267:25160–25166
33. Harris D, Aisen P (1973) Biochim Biophys Acta 329:156–158
34. Feig AL, Lippard SJ (1994) Chem Rev 94:759–805
35. Levi S, Salfeld J, Franceschinelli F, Cozzi A, Dorner MH, Arosio P (1989) Biochemistry 28:5179–5184
36. Yang C-Y, Meagher A, Huynh BH, Sayers DE, Theil EC (1987) Biochemistry 26:497–503
37. Wetz K, Crichton RR (1976) Eur J Biochem 61:545–550
38. Theil EC (1987) Annu Rev Biochem 56:289–315
39. Periera AS, Tavares P, Lloyd SG, Danger D, Edmondson DE, Theil EC, Huynh B-H (1997) Biochemistry 36:7917–7927
40. Sauer UH, Dao-pin S, Matthews BW (1992) J Biol Chem 267:2393–2399
41. Andrews SC, Harrison PM, Guest JR (1989) J Bacteriol 171:3940–3947
42. Le Brun NE, Wilson MT, Andrews SC, Guest JR, Harrison PM, Moore GR (1993) FEBS Lett 333:197–202